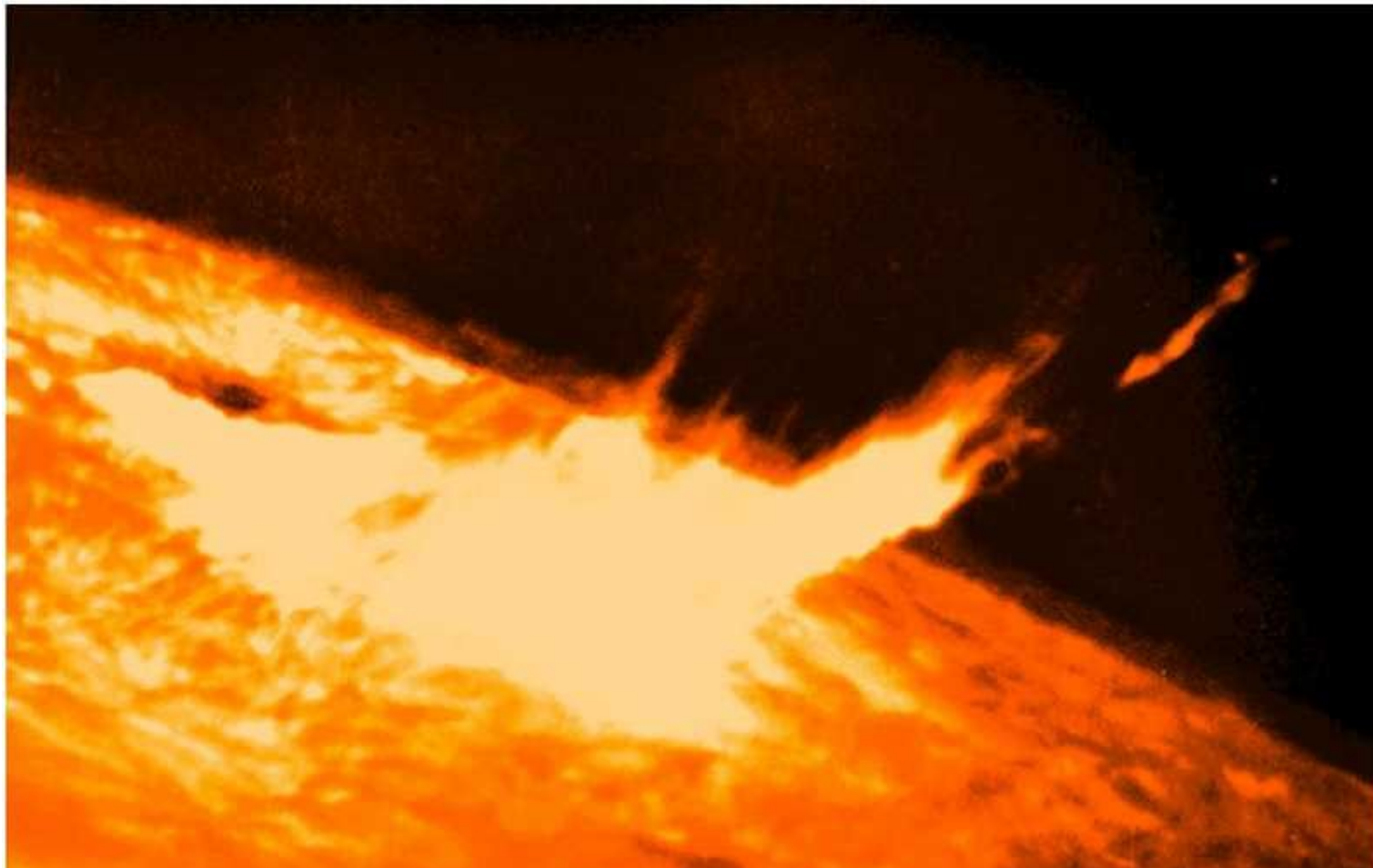
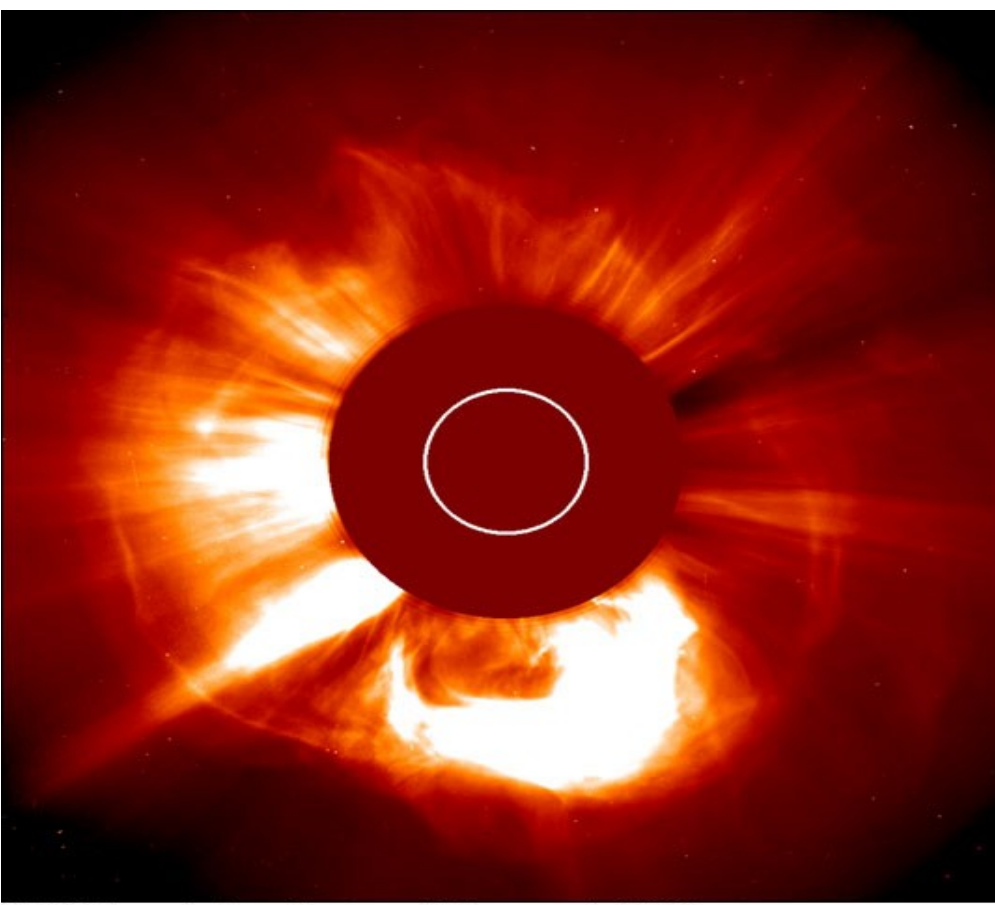


Solar Flares



Solar Flare

- A solar flare is a **sudden brightening** of solar atmosphere (photosphere, chromosphere and corona)
 - Flares release 10^{27} - 10^{32} ergs energy in tens of minutes.
(Note: one H-bomb: 10 million TNT = 5.0×10^{23} ergs)
 - A flare produces enhanced emission in all wavelengths across the EM spectrum, including radio, optical, UV, soft X-rays, hard X-rays, and γ -rays
- Flare emissions are caused by
 - hot plasma emitting in: radio, visible, UV, soft X-ray
 - non-thermal** energetic particles emitting in: radio, hard X-ray, γ -rays



11:30 UTC Large Angle and Spectrometric Coronagraph (LASCO)



14:24

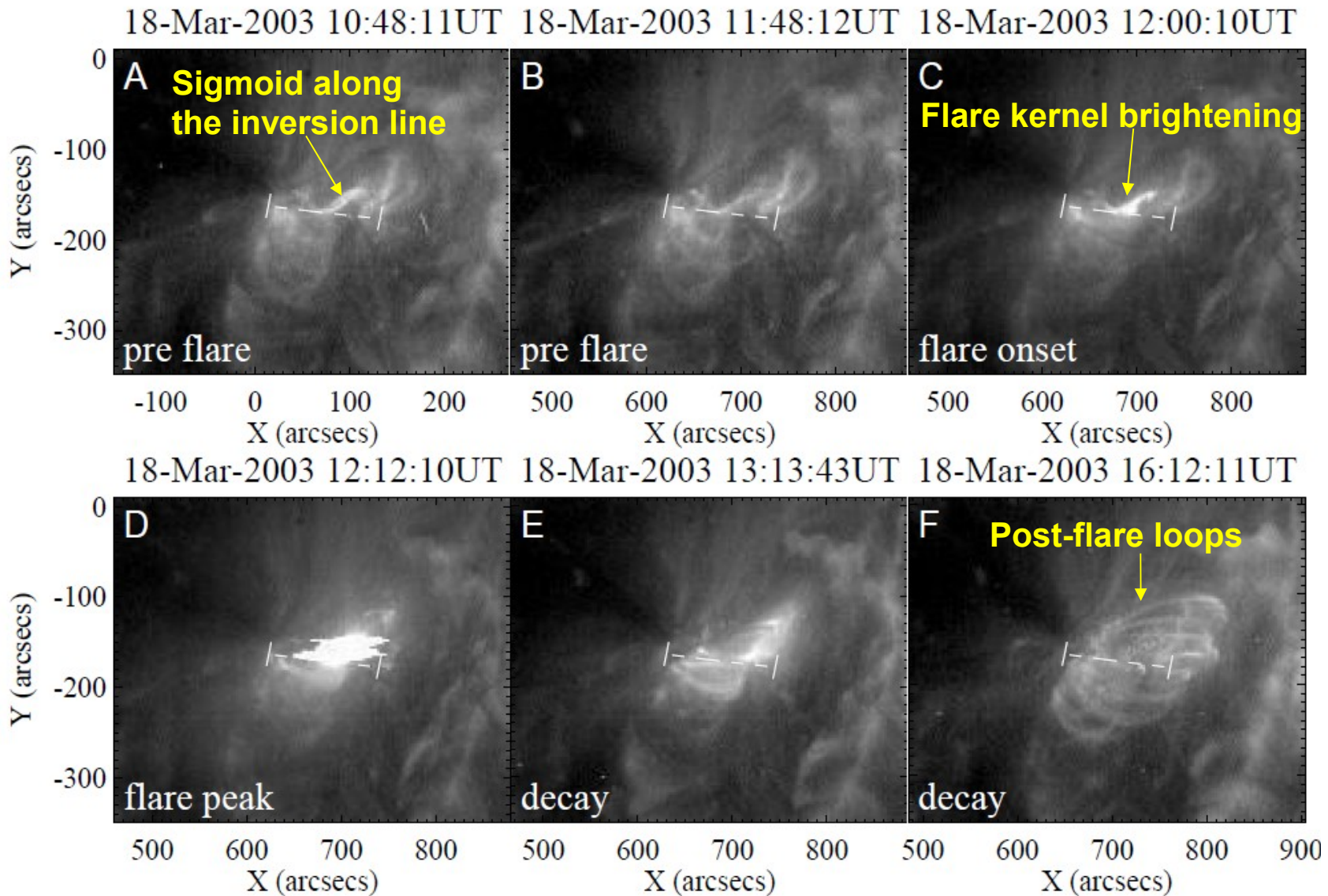
Michelson Doppler Imager (MDI)

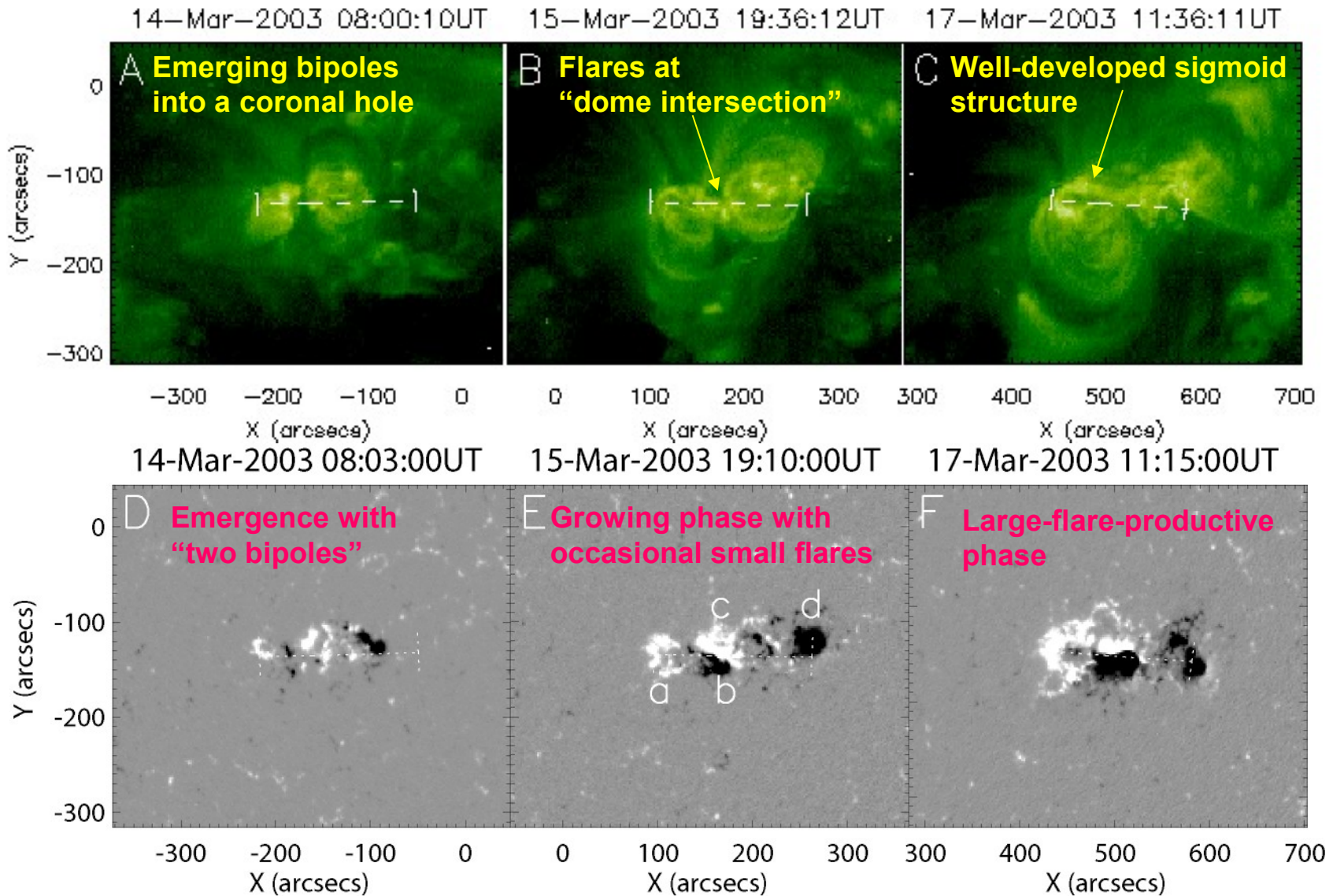


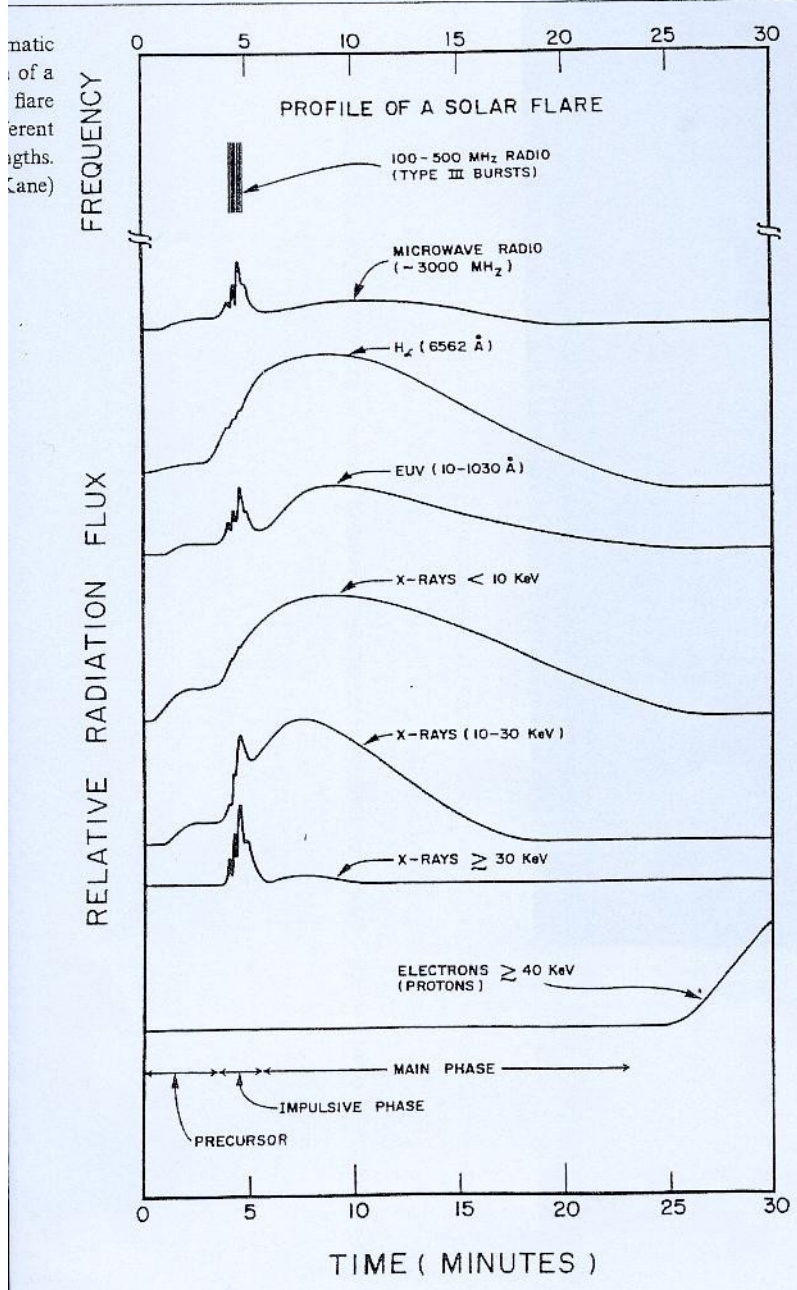
11:12 UTC

Extreme Ultraviolet Imaging Telescope (EIT)

Typical Flare Evolution in the Large-Flare-Productive Phase

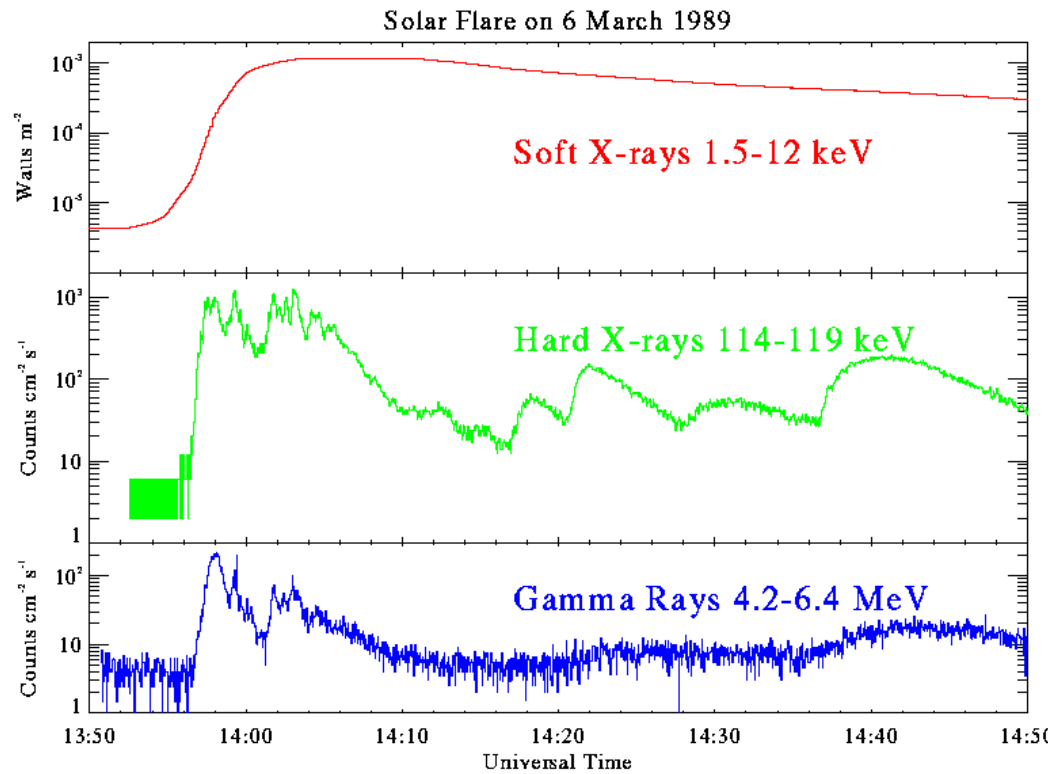






Flare: Temporal Evolution

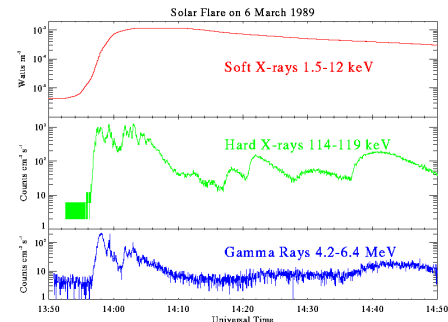
- A flare may have three phases:
 - **Preflare phase**: sometimes
 - **Impulsive phase**: e.g., 10 min from 13:56 UT – 14:06 UT
 - **Gradual phase**: e.g., many hours after 14:06 UT



- see Golub & Pasachoff, The Solar Corona, pag.288

Flare: Temporal Evolution

- **Pre-flare phase:** flare trigger phase leading to the major energy release. It shows slow increase of soft X-ray flux
- **Impulsive phase:** the flare main energy release phase. It is most evident in hard X-ray, γ -ray emission and radio microwave emission. The soft X-ray flux rises rapidly during this phase
- **Gradual phase:** no further emission in hard X-ray, and the soft X-ray flux starts to decrease gradually.
 - **Loop arcade** (or arch) starts to appear in this phase



Energy Source

$$E_{\text{th}} \approx 3nkTV = 10^{28} \text{ erg} \quad \text{for pre-flare } T = 10^6 \text{ K}$$

$$E_{\text{mag}} \approx (B^2/2\mu)V \approx 10^{32} \text{ erg}$$

Only **magnetic energy** (E_{mag}) is of the right order for the energy released in a large flare.

Potential and non-potential magnetic field

From Maxwell's equations (neglecting displacement current):

$$\text{curl } \mathbf{B} = \mathbf{J}$$

where \mathbf{B} = magnetic flux density and \mathbf{J} is the current.

When there is **no current**,

$$\text{curl } \mathbf{B} = 0, \quad \text{so } \mathbf{B} = \text{grad } \varphi$$

i.e. \mathbf{B} can be expressed in terms of a **potential** φ .

There is **zero energy available from a potential field**.

Flares derive their energy from **non-potential magnetic fields** (i.e. from currents).

1B11 MHD forces

The Magnetic Force F_M in a MHD plasma is $F_M = j \times B$.

Using the Maxwell equations:

$$F_M = \frac{1}{\mu_0} [(\nabla \times B) \times B] = -\nabla \left[\frac{B^2}{2\mu_0} \right] + \frac{1}{\mu_0} (B \cdot \nabla) B = \dots$$

And after a bit of lengthy algebra:

$$F_M = -\nabla_{\perp} \left[\frac{B^2}{2\mu_0} \right] + \frac{B^2}{\mu_0} \frac{R_C}{R_C^2}$$

R_c is the local radius of curvature of the field line. It points towards the centre of curvature of the field line.

Let us examine the two terms in the latter equation....

1B11 MHD forces: two simple components

$$\mathbf{F}_M = -\nabla_{\perp} \left[\frac{B^2}{2\mu_0} \right] + \frac{B^2}{\mu_0} \frac{\mathbf{R}_C}{R_C^2}$$

The magnetic force can be resolved into two conceptually simple components:

- A force perpendicular to the B-field which has the form of a pressure (it is the gradient of a scalar quantity $B^2/2\mu_0$), and
- A force towards the instantaneous centre of curvature that depends on: i) radius of curvature and ii) field strength B. This is equivalent to a tension force acting along the field lines.

Thus forcing the field lines together results in an opposing perpendicular pressure force, while trying to bend the field lines results in an opposing tension force.

1B11 MHD waves

This **magnetic pressure** and **magnetic tension** represent two kinds of restoring force that arise in a plasma in the presence of a magnetic field.

They are associated to wave modes: waves and perturbations that propagate in the plasma.

Most important ones:

- 1) **Alfven waves**
- 2) **Magnetosonic wave modes, in which both the magnetic field strength and the plasma pressure vary.**

1B11 MHD waves

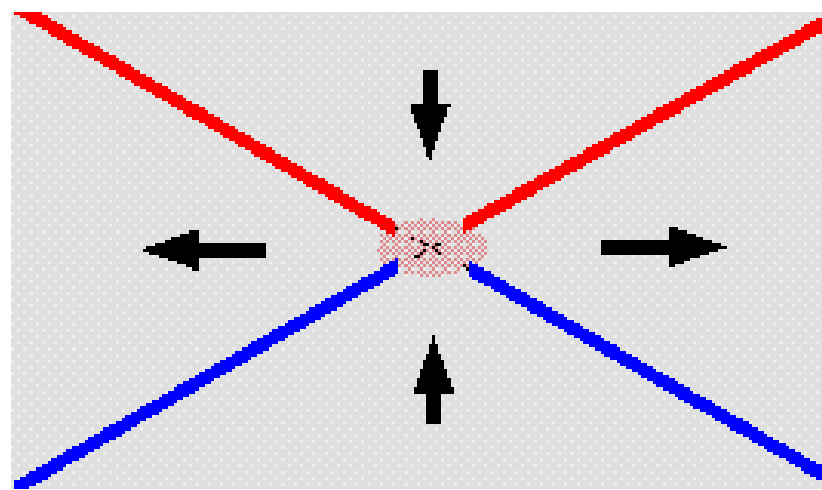
The Alfvén wave is a very important one. It is entirely due to the tension force associated with the magnetic field.

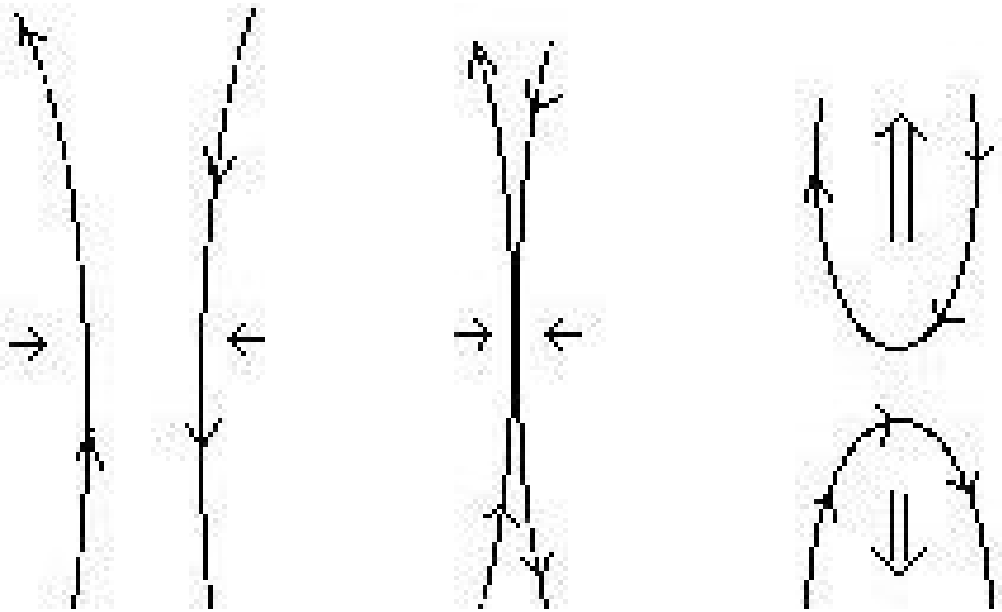
- It is essentially a magnetic wave, as there is no associated compression of the plasma as in the case of sonic (pressure) waves.
- It propagates preferentially along the field direction (and not across it) with speed: $V_A = -B^2 / \sqrt{\mu_0 \rho}$

Magnetic Reconnection

Magnetic Reconnection

- Magnetic fields with opposite polarities are pushed together
- At the boundary, $\mathbf{B} \rightarrow 0$.
 - Called **diffusion region**, since plasma could cross \mathbf{B}





A simple example of magnetic reconnection.

Two field lines of opposing polarity are forced together.

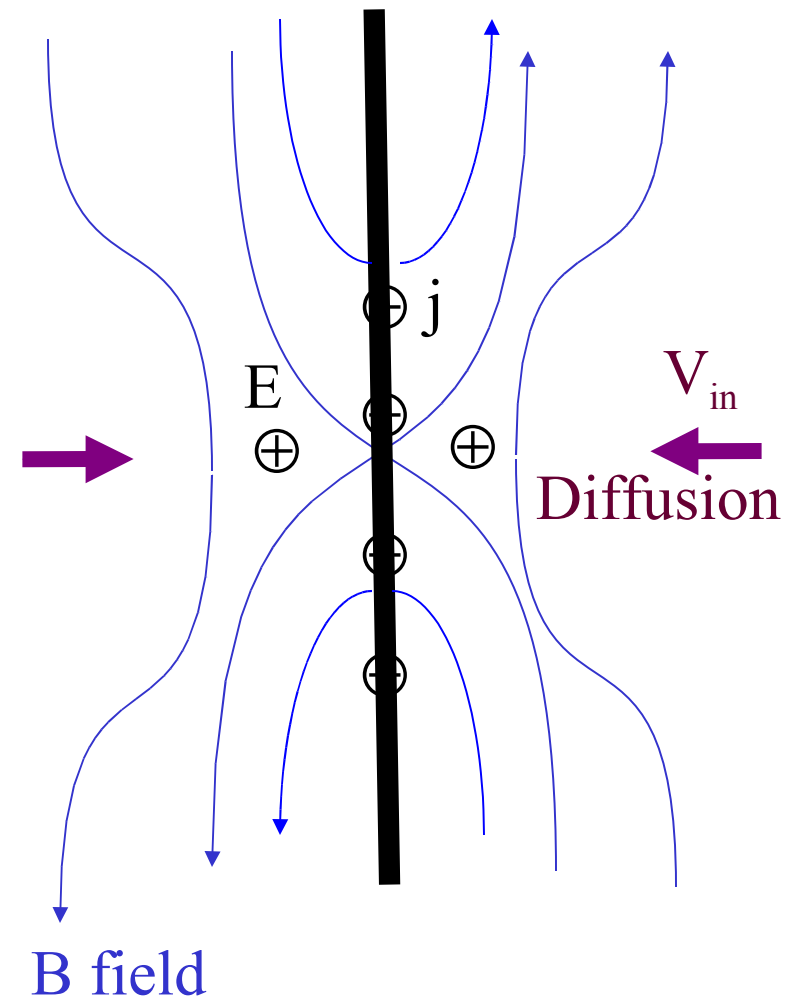
When they meet they reconnect and snap back into a lower energy configuration.

The upper loop is ejected into space, dragging plasma with it.

1B11 Magnetic reconnection

If there is a strong B-field gradient and the fields on either side of the gradient are anti-parallel, then diffusion of the field at the gradient can lead to a loss of total magnetic flux
→ this situation is called magnetic annihilation.

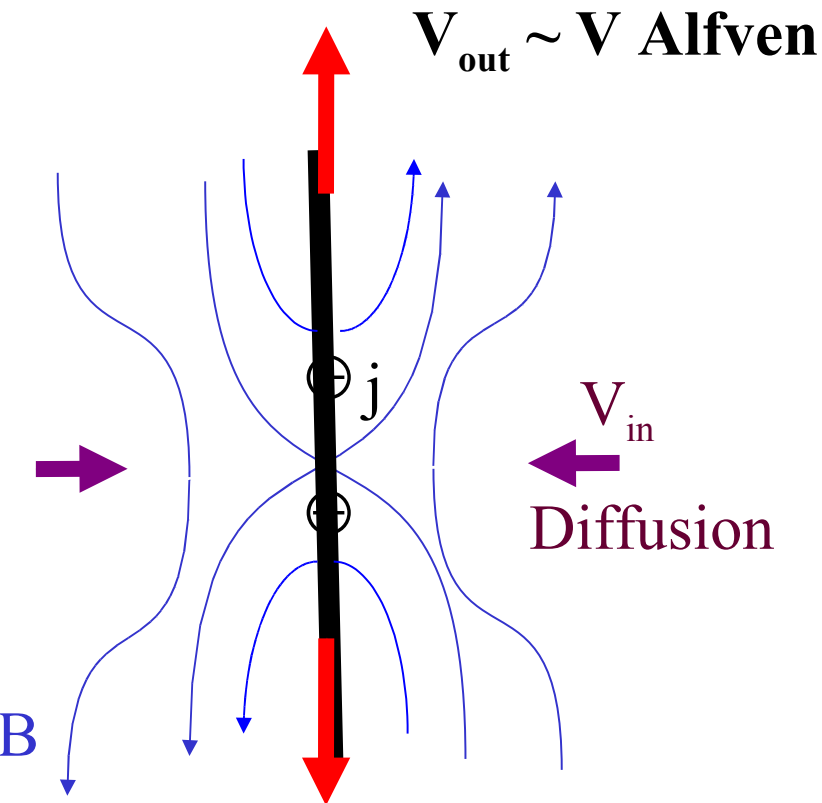
Field lines are convected into the diffusion region and merge with field lines with opposite orientation (which originally were on the other side of the gradient)



1B11 Magnetic reconnection

The resulting “reconnected lines” are sharply bent through the current sheet.

Magnetic tension forces associated with these bent lines accelerate the plasma along the current sheet and away from the diffusion region on each side.



The simplest magnetic reconnection geometry. Anti-parallel field lines are separated by a thin current sheet (light grey) across which the field reverses. Due to the small scale lengths, the frozen-in flux approximation breaks down → magnetic flux diffuse from both sides. The field reconnects to form 2 hairpin like field lines, which rapidly contract away from the neutral “X”-point. Outflows jets of plasma are formed, also moving away from the “X”-point, on both sides.

Magnetic merging - reconnection

$$\partial \mathbf{B} / \partial t = \nabla^2 \mathbf{B} / (\sigma \mu_0) + \text{curl}(\mathbf{v} \times \mathbf{B})$$

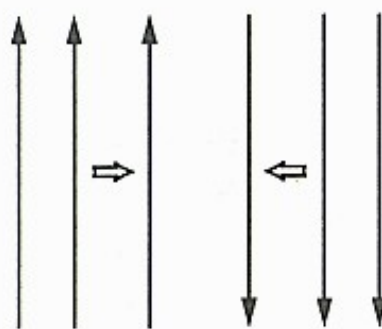
**Rate of change of field in a flare volume =
diffusive term + convective term.**

Get an order-of-magnitude estimate of quantities by approximating $\partial / \partial t = 1 / t$, $\text{curl} = 1 / L$, $\nabla^2 = 1 / L^2$:

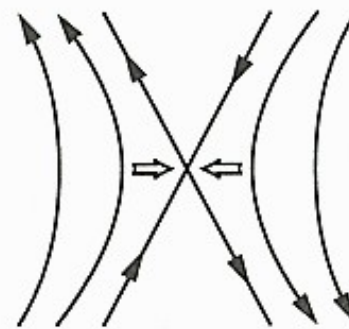
If there is no convective term, then: $B / \tau_D = B / (L^2 \sigma \mu_0)$

or **diffusion time**, $\tau_D = L^2 \sigma \mu_0$. (4)

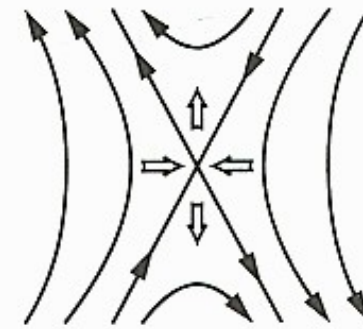
Field lines form \longrightarrow *X-point and separatrix (curved surfaces in space that divide different bundles of flux.)*.



$t < 0$



$t = 0$



$t > 0$

small spatial lengths!

the magnetic Reynolds number within the current sheet
may be relatively small:

→ diffusion of the magnetic field through the plasma
start to be important!

The basic problem is that high-temperature coronal plasma, especially for flares, **has an extremely large electrical conductivity σ** (comparable to the conductivity of solid copper at room temperature).

So the energy release timescale appears to be of the order of **years** rather than the **observed seconds** or minutes.

diffusion time, $\tau_D = L^2 \sigma \mu_0$

The “classical” value of conductivity is

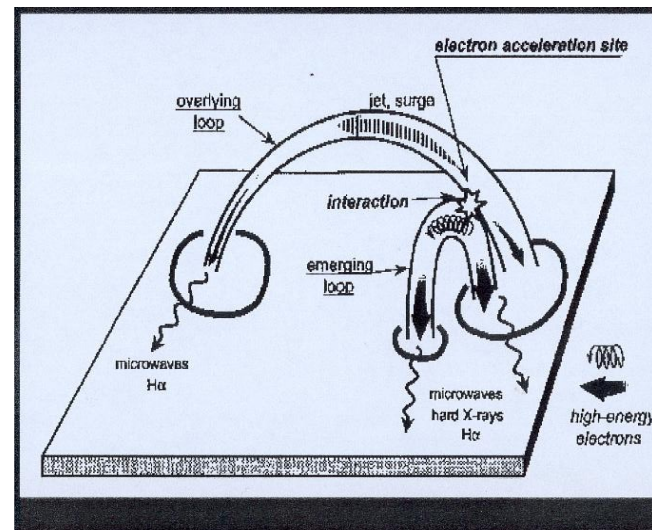
$$\sigma = 10^{-3} T_e^{3/2} \text{ S.I. units}$$

where T_e = electron temperature. For the quiet corona, $T_e = 2 \text{ MK}$,
so $\sigma = 2.8 \times 10^6 \text{ S.I. units}$.

(Solid copper has $\sigma = 5 \times 10^7 \text{ S.I. units}$.)

So the diffusive time scale τ_D for the pre-flare volume (take this to be $L = 1,000 \text{ km} = 10^6 \text{ m}$) is possibly as high as $\sim 3 \cdot 10^{12} \text{ s}$ (billions of years).

However, **these simple estimates must be wrong** for actual flares. It is likely that **$L \sim \text{a few metres}$** , not the observed flare dimensions which represent the “aftermath” of a flare, not the magnetic field diffusion region.



Diffusion Region

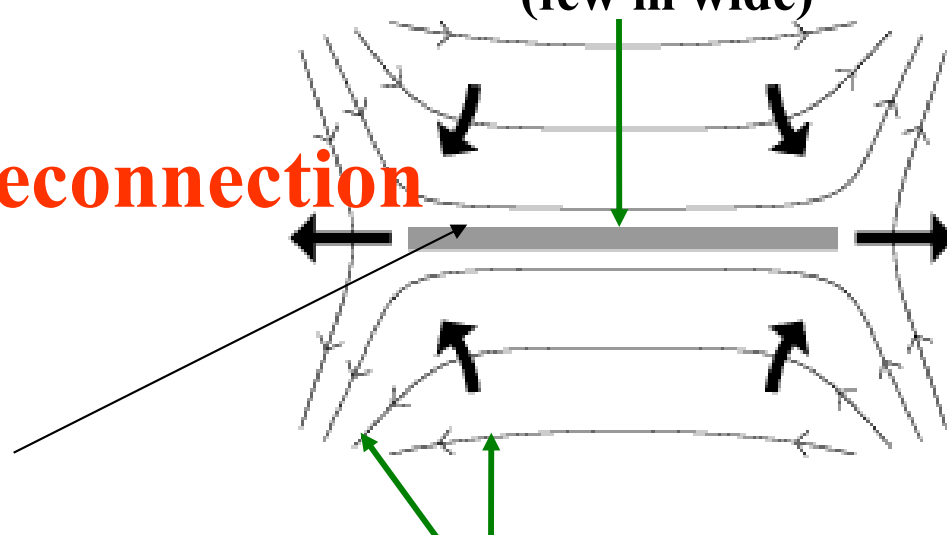
X-type reconnection

Reconnection region

(few m wide)

Field lines

Plasma flow:
reconnection
“jet”

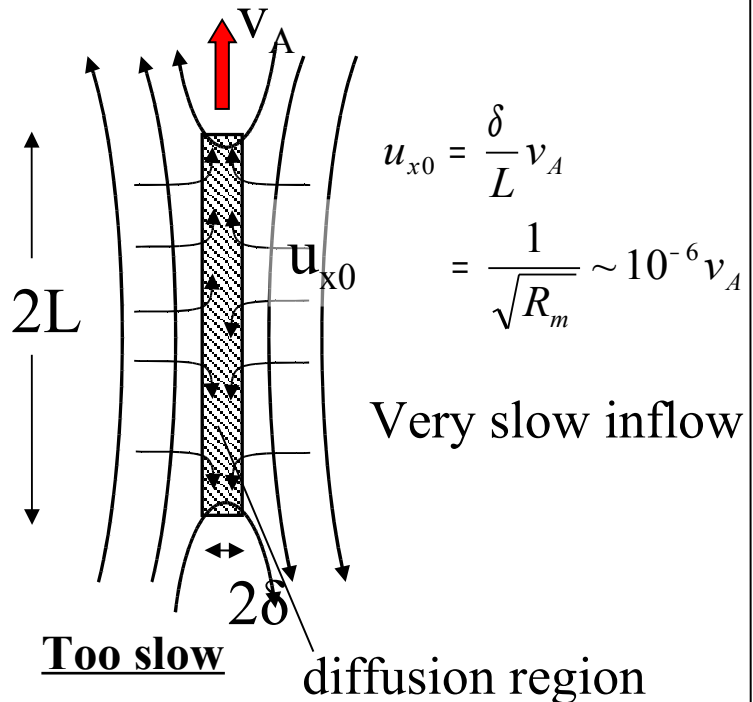


Limit: gyroradius of electrons

Petschek reconnection takes place

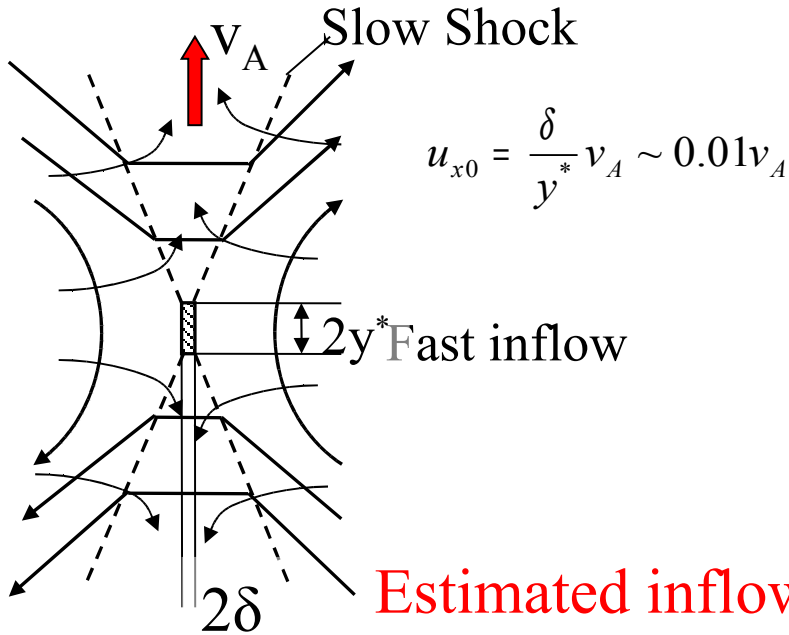
Sweet-Parker

Inflow goes through diffusion region.



Petschek

Inflow goes through slow shock,
bypassing diffusion region.



Estimated inflow speed
 $0.07v_A$ (Tsuneta 1996)
 $0.03v_A$ (Yokoyama 2001)

diffusion time,

$$\tau_D = L^2 \sigma \mu_0.$$

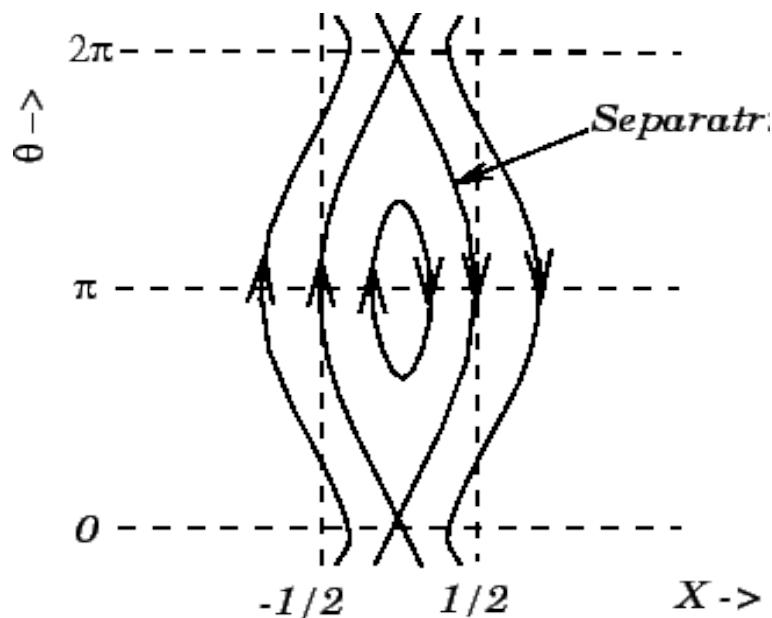
Petschek reconnection occurs if the anomalous resistivity sets in on the current sheet .

Possible only for peculiar current sheet thickness

current sheet thinning via the "fractal tearing instability" (Tanuma 2000; Shibata & Tanuma 2001; Tanuma et al. 2001a).

the tearing mode gives rise to the formation of a magnetic island.

Field-lines inside the separatrix have been broken and reconnected, and now possess quite different topology.

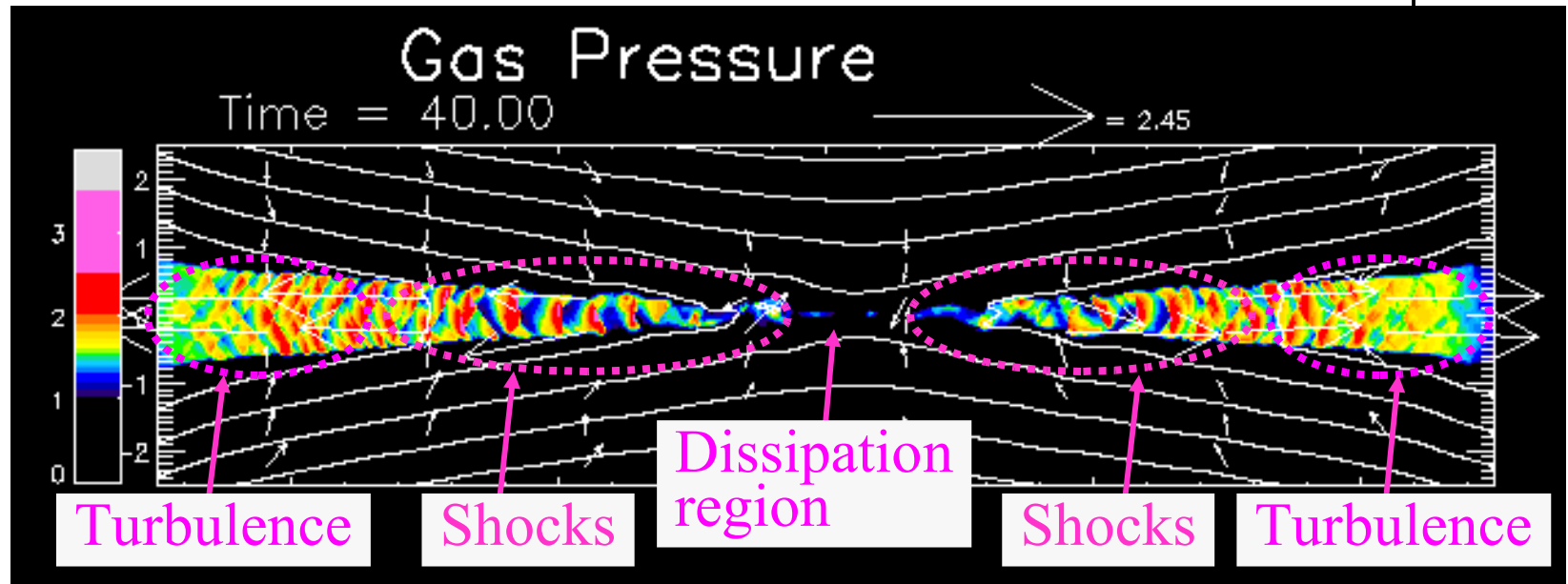
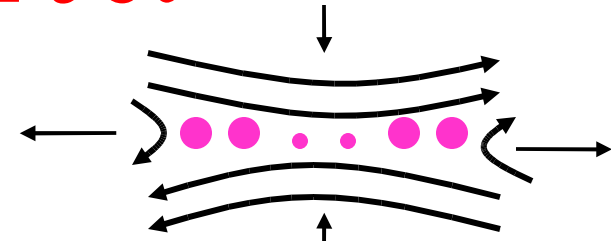


Both the tearing-type and the Petschek-type reconnections develop from an initially antiparallel magnetic field.

In the tearing-type field geometry the current-sheet plasma, accelerated at X-type neutral points through reconnection, cannot be ejected away from the system but is confined in the resulting magnetic islands.

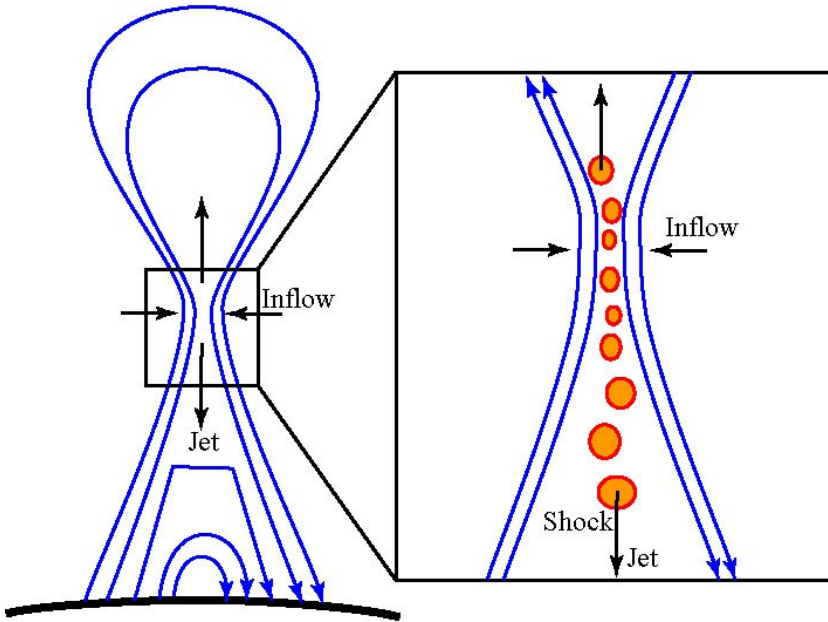
On the other hand, in the Petschek-type field geometry the plasma can freely be ejected away from the system, so that the antiparallel field is allowed to collapse into the X-type neutral point.

Internal Shocks in the Reconnection Jet in Solar Flares



S.Tanuma & K.Shibata
(Kwasan Observatory, Kyoto University)

Internal Shocks in Reconnection Jet



- We suggest that the internal shocks could be created in the reconnection jet by the secondary tearing instability.
- And the energetic electrons could be accelerated in the internal shocks.

Tearing Instability

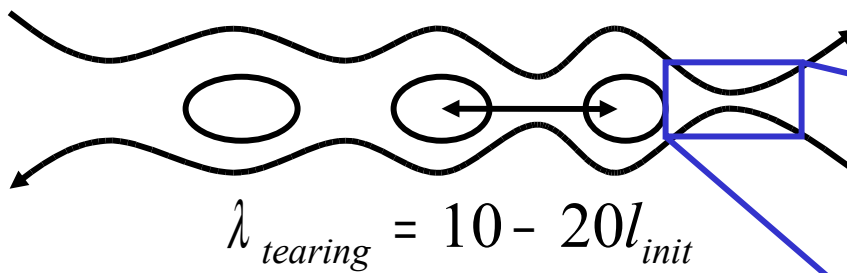
1. Initial current sheet



$$\tau_{tearing}^{init} \approx (\tau_A^{init} \tau_d^{init})^{1/2}$$

A resistivity (η_0) **tears** the current sheet.

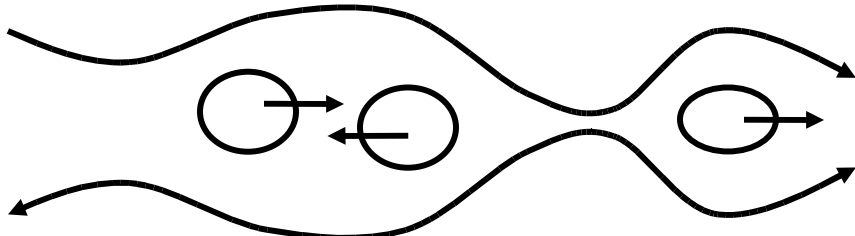
2. Linear \rightarrow Nonlinear



$$\lambda_{tearing} = 10 - 20 l_{init}$$

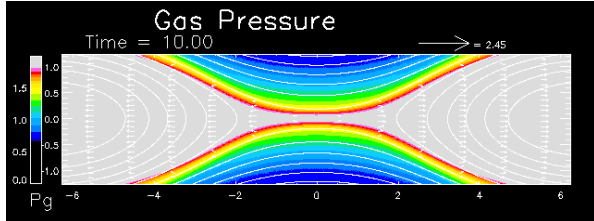
$$\approx \left(\frac{l_{init}^3}{\eta_0 v_A^{init}} \right)^{1/2}$$

3. Nonlinear \rightarrow Plasmoid-ejection

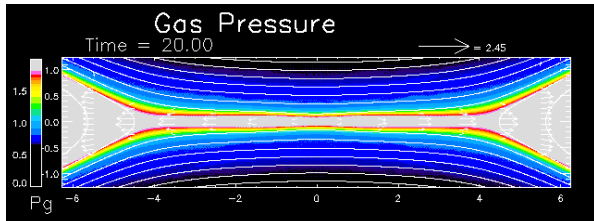


The sheet becomes much thin by the secondary tearing instability so that anomalous resistivity is enhanced and the fast reconnection starts.

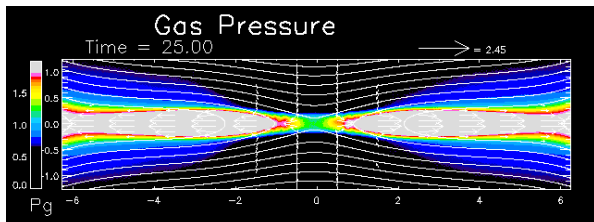
Simulation Results (Internal Shocks)



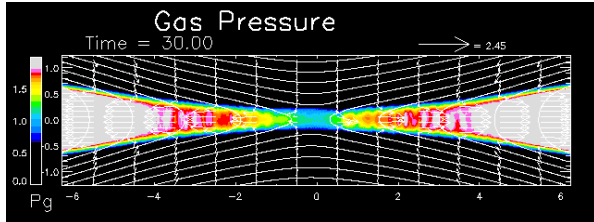
*The current sheet thinning by the tearing instability



*Slow (Sweet-Parker-like) reconnection and further thinning by secondary tearing instability

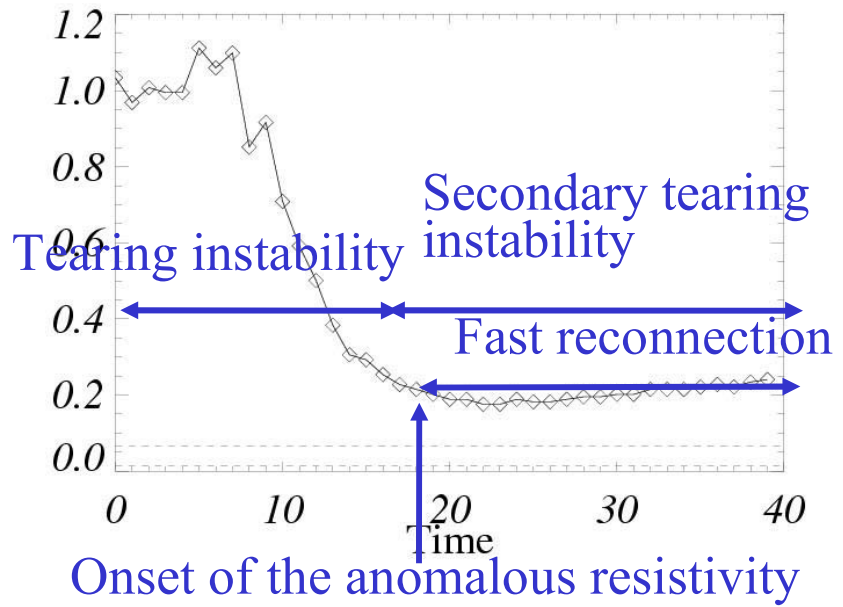


*The onset of the anomalous resistivity



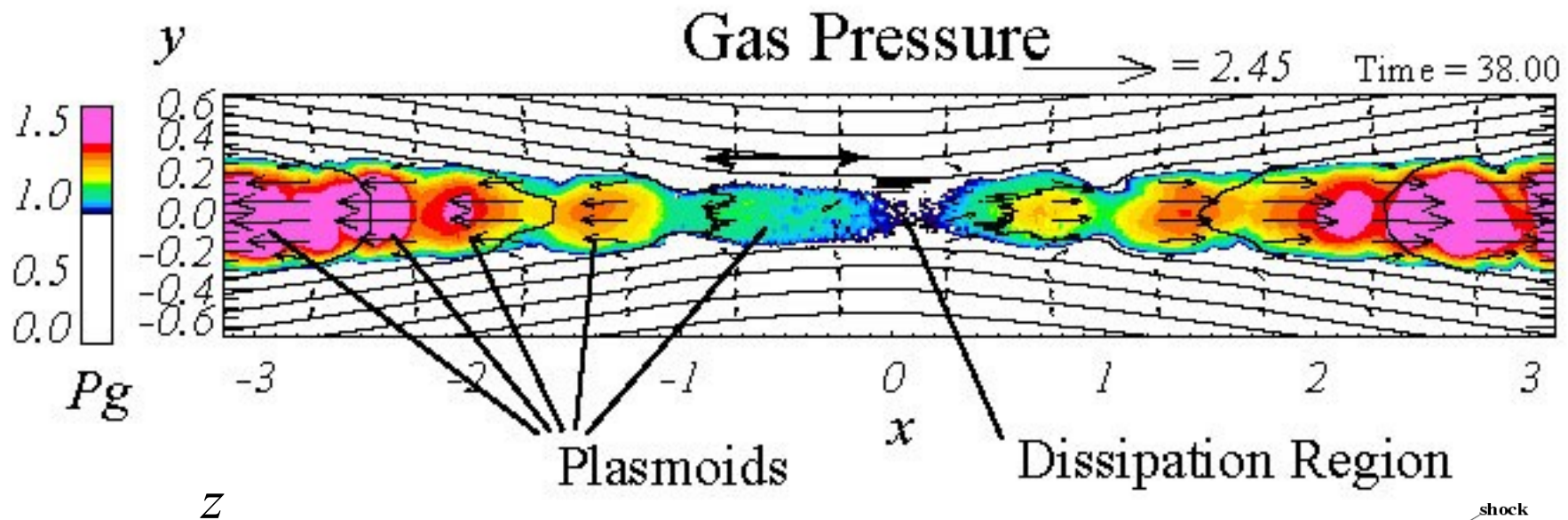
*Fast (Petschek-like) reconnection and multiple fast shocks

Time variation of
current sheet half-thickness



Creation of Plasmoids

Many plasmoids are created (O-points) by the secondary tearing instability in the diffusion region and ejected



S.Tanuma & K.Shibata

“..As the results, we find that many plasmoids are created by the secondary tearing instability.

They are ejected, and the multiple fast shocks are created.“

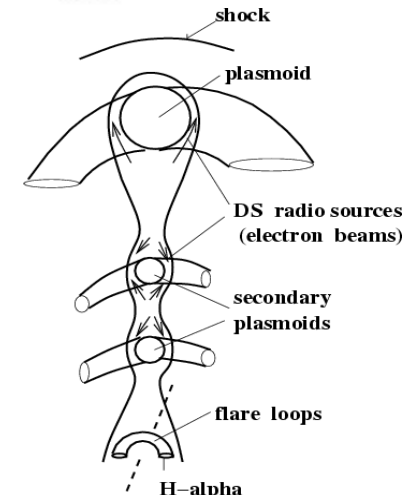


(Fig: Karlicky 2004)